Climate and early karstification: What can be learned by models?

WOLFGANG DREYBRODT [1] & FRANCI GABROVSEK [1,2]

[1] *Karst Processes Research Group, Institute of Experimental Physics,
University of Bremen, D-28334 Bremen, Germany*
[2] *Karst Research Institute, ZRC-SAZU, Postojna, Slowenia*

ABSTRACT:

DREYBRODT, W. & GABROVSEK, F. 2002. Climate and early karstification: What can be learned by models? *Acta Geologica Polonica*, **52** (1), 1-11. Warszawa.

First an overview is given on the present state of modelling of karst aquifers and karst conduits. Emphasis is placed to early karstification in rock massives with low fissure density as suggested for states 1 and 2 in Ford's four-state-model. In this case early karstification proceeds under the condition of a constant hydraulic head. The evolution of a single isolated karst conduit, as well as evolution of karst conduits in two-dimensional networks of fractures are discussed. From these models the parameters determining early karstification can be identified. These are the initial aperture widths of the fractures, their lengths, the hydraulic head, and the viscosity of water, as well as the parameters of the non-linear dissolution kinetics of limestone, and the equilibrium concentration of calcium with respect to calcite. Early karstification under constant head conditions is characterized by a feedback-mechanism which couples flow rates through the conduits to the dissolutional widening of the fracture. After an initially slow increase in flow and in aperture width of the fracture a dramatical increase of flow rates and fracture widening occurs at breakthrough. The breakthrough time, when this event happens can be quantified from the parameters defined above. This time can be considered as a measure of intensity of karstification. Large scale climatic parameters, especially temperature exert influence to breakthrough time. Under otherwise identical geological conditions breakthrough times in tropic and moderate climates are about 5 times shorter than in arctic/alpine climate. Micro-climatic conditions, however, are of similar importance. If the vegetation on a karst plateau exhibits regions with different CO_2 partial pressure in the soil, waters from these differing regions may mix at fracture-confluences in the karst massive. Mixing corrosion causes renewed solutional power at these confluences. Therefore breakthrough times can be reduced significantly. We present details of this mechanism and its influence to breakthrough times. Already moderate differences in in differently vegetated areas are sufficient to reduce breakthrough times by a factor of four. Although macro- and micro-climatic variables exert a significant influence to karstification it is not possible to draw conclusions on climatic conditions from the structure of a karst aquifer in retrospective.

Key words: Karst, Early karstification, Modelling, Climate.

INTRODUCTION

To understand the genesis of caves and karst aquifers has been an object of research from the beginning of the last century. Many apparently conflicting theories have been discussed, which were based on a descriptive point of view. In 1932 SWINNERTON introduced a water table model of speleogenesis, with a stationary water table. Cave evolution in this model propagates along the pathway with the least hydraulic resistance from the input to the output, creating a cave evolving towards the spring. A different view was taken

in by RHOADES & SINANCOURI (1941). They no longer regarded the watertable as fixed, but they recognized that the water table could decline steadily due to enlargement of fissures close to it by the dissolving action of the water. In their model the watertable is progressively lowered to base level and a cave propagates headwards. For an overview of the early speleogenetic models see FORD (1999). FORD (1971), FORD & EWERS (1978) and FORD & WILLIAMS (1989) in iterative steps suggested a four-state model. In this model the permeability of the karstifying rock determines the routes of the entering water. If only few but deep reaching fractures are present the water table will be high and caves evolve under constant head conditions as suggested by SWINNERTON. As a result deep bathyphreatic caves originate. On the other extreme, a highly fissured rock massive with low permeability will exhibit a low, ideal water table close to base level and a water table cave originates. Thus the four-state model comprises different boundary conditions of karst aquifers evolution and implicitly reconciles the former conflicting views.

With increasing knowledge on the equilibrium chemistry of the system H_2O-CO_2-$CaCO_3$ and its dissolution kinetics [for an overview see DREYBRODT (1988) or DREYBRODT (2000), and DREYBRODT & EISENLOHR (2000)] first computer models of cave origin were provided by DREYBRODT (1988, 1990, 1996) and PALMER (1991). These first models described the evolution of karst conduits along one-dimensional channels, through which calcite aggressive water is driven by a constant head acting between input and output.

An essential ingredient to these models is the realisation that the dissolution kinetics of limestone in a H_2O-CO_2 solution switches to a nonlinear rate law at concentrations of Ca above 70-90% of its equilibrium concentration with respect to calcite. This provides a feed back mechanism by which increasing flow rates cause increasing dissolution along the conduit and particularly at its exit and vice-versa (DREYBRODT 1996, DREYBRODT & GABROVSEK 2000a, GABROVSEK 2000). As a consequence flow rates through the initial conduit and its enlargement first proceed slowly, but then are accelerated until a breakthrough event occurs with a dramatic increase of widening and flow. From then on the constant head conditions break down and further evolution of the conduit is determined by the amount of water available at the input, or in other words constant recharge conditions. It should be noted at that point that the basic ingredient, that is the nonlinearity of the dissolution rates as a function of undersaturation, was first recognized qualitatively by WHITE (1977) and PALMER (1984). They realized that a sufficient amount of conduit widening at the exit of the initially narrow fracture with

an aperture width of about 0.1 mm can only be provided by non-linear kinetics of limestone dissolution. As a major advance these first digital models provided first realistic numbers of scales in time and length of cave evolution, relying only on experimental data of limestone dissolution and on well defined physical parameters, such as the initial aperture width of the fracture, the hydraulic head acting, and the length of the fracture.

The evolution of one-dimensional conduits is a basic element of karst modelling. All later two-dimensional models contain one-dimensional fractures with known head differences, and Ca-concentrations of the water entering them. The second ingredient to such models is to calculate the flow rates in each of its fractures under laminar or turbulent flow conditions. Two-dimensional models of aquifer evolution under constant head conditions have been reported by GROVES & HOWARD (1994) and HOWARD & GROVES (1995). These models have been refined on larger 2-D percolation networks by SIEMERS & DREYBRODT (1998), GABROVSEK & DREYBRODT (2000a), GABROVSEK (2000), and KAUFMANN & BRAUN (1999).

Text-fig. 1 presents an overview of the different modelling approaches. (1) shows a single isolated conduit evolving under constant head conditions with water input from a river at the plateau at head h_{in} and the spring at head h_{out} in the valley. (2) depicts a two-
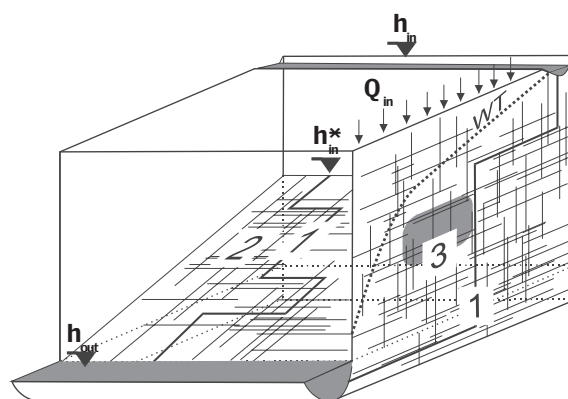

Fig. 1. The elements of a karst aquifer discussed in this work. **1 –** A single fracture under constant head conditions. **2 –** 2D fracture network under constant head conditions. **3 –** Vertical section of an unconfined aquifer with a constant recharge and constant head conditions applied to it. As shown, a dense network of fine fractures and a coarse network of prominent fractures are superimposed to simulate the multiple porosity character of karst aquifers. The thick dashed line WT represents the position of the water-table. The hydraulic heads at the inputs and outputs are denoted as h_{in}, $h_{in}*$ and h_{out}

dimensional network of fractures (light lines) in a plane. From the many competing pathways only a few are selected. The fat line shows one of them. Under constant head conditions the water table WT remains fixed until breakthrough. The light lines in the figure are prominent fractures with aperture widths of several tenths of a millimetre. They are widely spaced and embedded into a dense net of fine fractures (3) with aperture widths below 0.1 mm. More realistic models have to take into account that water can be exchanged between the net of prominent fractures and the dense network of fine fractures. Such models have been recently published by CLEMENS & *al.* (1997), KAUFMANN & BRAUN (2000), and GABROVSEK & DREYBRODT (2001). In the models of CLEMENS & *al.* and KAUFMANN & BRAUN the hydraulic conductivity of the dense network is taken in the order of $10^{-5} ms^{-1}$, and constant recharge conditions of about 450 mm/year are assumed. Dissolution is taken to be active in the prominent fractures solely. When these become enlarged they drain the dense fracture part of the aquifer, thus providing a feedback, concentrating flow to the evolving conduits. Therefore these models simulate karstification of initially highly permeable rock close to state 4 of Ford's model.

In this work we restrict to the evolution of caves in state 1 or 2 of Ford's four-state model, where flow is mainly along prominent fractures and constant head conditions prevail. In other words we neglect the dense fracture net and regard the early state of karstification until breakthrough. Under these assumptions the parameters determining karstification are limited and it is possible to discuss the influence of climatic parameters on the early stage of karst genesis. It should be stressed again that the conclusions drawn are restricted to the evolution of state 1 and 2 aquifers where constant head conditions are present. After presenting the results for one-dimensional conduits and two-dimensional nets, we will discuss the influence of climate to karstification in such geological settings.

EVOLUTION OF ONE-DIMENSIONAL CONDUITS

Text-fig. 2 depicts an alternative representation of case (1) in Text-fig. 1. It schematically illustrates an uplifted limestone block, which is dissected by various primary fractures such as joints and bedding planes at the onset of karstification. Some of these comprise percolating pathways from the upper surface to a valley. Through these, the surface water present at some input points at the top is driven down to the valley. The solutional attack of this CO_2-containing water widens these
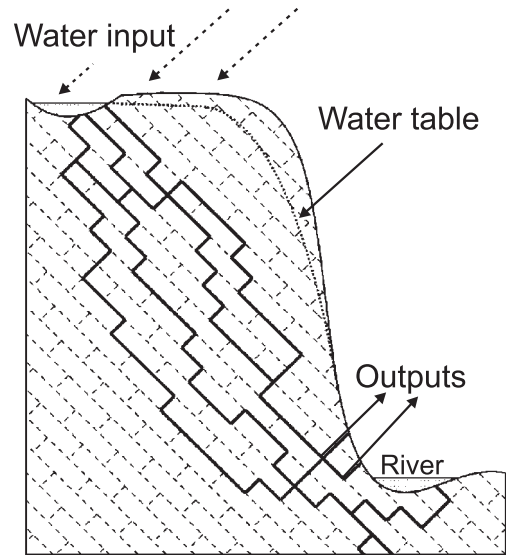

Fig. 2. Schematic drawing of a karst aquifer in its initial state. The full lines represent a net of percolating pathways consisting of narrow initial fractures which transmit water from the input to the outputs

fractures by chemical dissolution of the bedrock and underground drainage networks may result (DREYBRODT 1988, FORD & WILLIAMS 1989, WHITE 1988). To understand the evolution of karstification on its scales in space and time one has to specify by which parameters these processes are determined. To this end first models have been put forward during the last decade (DREYBRODT 1988, 1990, 1996; DREYBRODT & GABROVSEK 2000; GABROVSEK 2000; PALMER 1991, 2000), which investigate the evolution of the aperture widths of a one-dimensional fracture with initial even spacing. They all replace the complicated natural fractures by a plane parallel fracture of length L, initial aperture width a_0 of a few tenths of a millimeter, and width b_0 in the order of meters. The hydraulic head h acting at the entrance drives CO_2-containing, calcite aggressive water through this fracture, thus widening its aperture by dissolution. The rates at which this happens are governed by the dissolution kinetics of limestone, which are given by

$$F(c) = k_1(1 - c / c_{eq}) \quad \text{for} \quad c < c_s \qquad (1a)$$

and

$$F(c) = k_n(1 - c / c_{eq})^n \quad \text{for} \quad c \geq c_s \qquad (1b)$$

k_1 and k_n are rate constants in mole/cm^{2}s, c is the concentration of ions and c_{eq} their equilibrium concentration with respect to calcite in mole/cm^3. At the concentration c_s, the rates switch from a linear rate law to higher order kinetics with exponent n. Depending on the lithology of the specific limestone n varies between

3 and 11 (SVENSSON & DREYBRODT 1992). The switch concentration c_s is about $0.7c_{eq}$ to $0.9c_{eq}$. This rate law has first been suggested by PALMER (1984), and later experimentally proven to be valid for dissolution of limestone under the conditions of a closed system with respect to CO_2, as it occurs in a completely water filled fracture (SVENSSON & DREYBRODT 1992; EISENLOHR & al. 1999). It must be stressed at this point that this non-linear rate law is essential to the evolution of karst. Under the action of solely a linear rate law, karstification cannot proceed in geological time scales (DREYBRODT & GABROVSEK 2000).

Text-fig. 3 shows the evolution of a one-dimensional karst conduit with an initial aperture width of $a_0 = 0.02$ cm, $b_0 = 100$ cm, $L = 10^5$ cm, and a hydraulic gradient i $= h/L = 0.05$. The equilibrium concentration is $c_{eq} = 2 \cdot 10^{-6}$ mole/cm^3 as it commonly occurs in karst waters. The inflowing solution has a concentration c = 0. The rate constants $k_1 = 4 \cdot 10^{-11}$ mole/cm^{2}s, and $k_n = 4 \cdot 10^{-8}$ mole/cm^{2}s are typical values obtained from laboratory experiments under the conditions of a closed system at 10°C (DREYBRODT & EISENLOHR, 2000, EISENLOHR & al. 1999). We refer to this as the standard later on.

Text-fig. 3a in a logarithmic plot depicts the flow rates through the fracture as a function of time. Initially there is a slow increase which is enhanced in time until the flow rates are drastically accelerated to such an amount that they exceed the water available at the surface (cf. Text-fig. 2). At this breakthrough time T_B the hydraulic head breaks down and the initial phase of laminar flow through the fracture is terminated.

Text-fig. 3b represents the evolution of the aperture widths along the fracture for various times. During the first 90% of T_B, widening of the fracture is restricted to its entrance, and only a slow increase of its aperture width is observed at the exit, until close to breakthrough a dramatically widening occurs. This behavior is mirrored by Text-fig. 3c, which shows the concentration of Ca^+ along the fracture (note the logarithmic scale). During most of the time it rises quickly at the entrance until c_S is achieved after a short distance compared to the length. From thereon higher order dissolution kinetics, active along almost the entire length of the fracture, determines the evolution of its aperture width. Then, at breakthrough, the concentration drops to a value close to zero. Further dissolution is then governed by the first order kinetics and widening is uniform along the entire fracture. Text-fig. 3d depicts the dissolution rates along the fracture. In the region of linear kinetics (cf. eqn. 1a) close to the entrance the rates
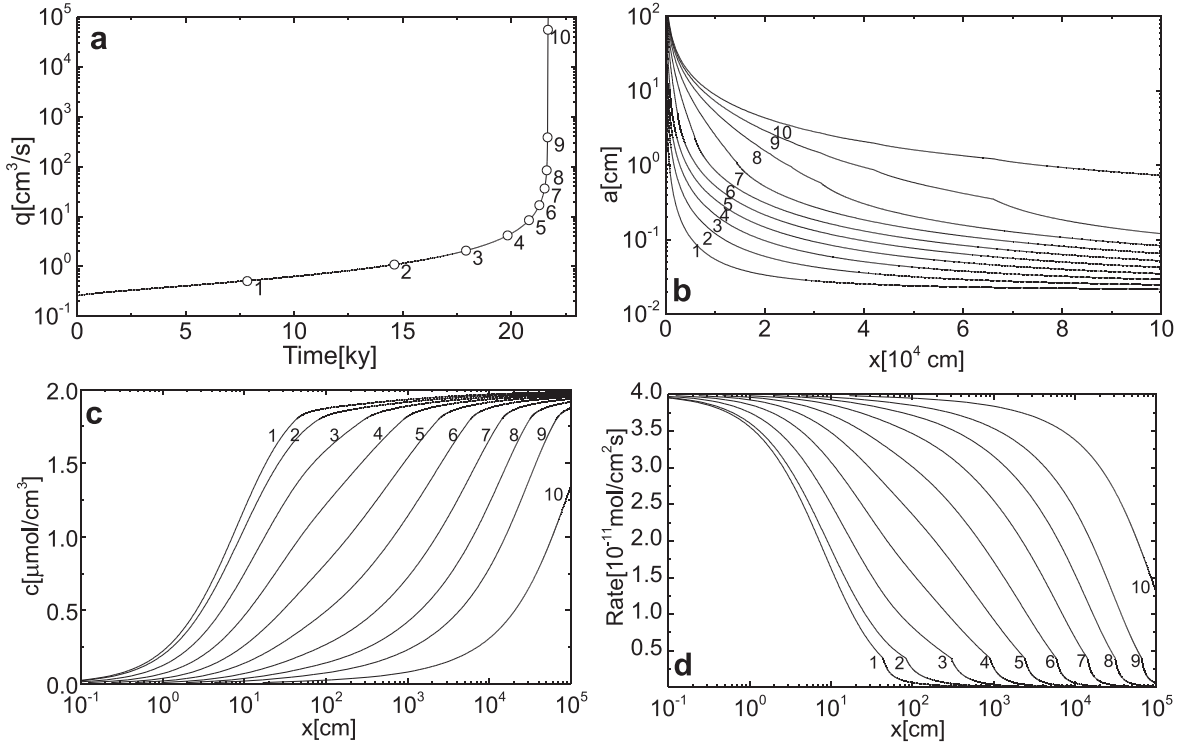

Fig. 3. Evolution of a single fracture in time and space: numerical results. **a** – Evolution of the flow rate in time. Open circles denote the times when profiles in figures b, c and d were recorded. **b** – Evolution of aperture widths. Note the logarithmic scale for a. **c** – Evolution of concentration. **d** – Evolution of dissolution rates. Note the logarithmic scale for x in figures b and c. Profiles are recorded each time the flow rate doubles

drop exponentially, as long as first order kinetics is active. Beyond the point c_S where the rates are nonlinear (cf. eqn. 1b), they drop much slower with a hyperbolic law, such that a small but still significant dissolutional widening exists at the exit. The rates at the exit increase with time due to increasing flow, and the region of first order dissolution slowly penetrates into the fracture with accelerated speed, until breakthrough occurs. Details of this dynamic behavior are given in the literature (DREYBRODT 1996, 1998; DREYBRODT & GABROVSEK 2000a).

It should be noted at this point that this behavior is not affected as long as the inflowing solution has a finite concentration $c_0 \leq c_S$, since during 90% of the time needed for breakthrough the higher order kinetics is active along almost entire length of the fracture (DREYBRODT & GABROVSEK 2000a, DREYBRODT 1996). The time to achieve breakthrough is governed by a positive feedback mechanism. Widening at the exit increases flow rates due to the Hagen-Poisseuille law of laminar flow with approximately $a^3(L,t)$, where $a(L,t)$ is the aperture width at the exit. This increased rate enhances the dissolution rate at the exit thus causing further acceleration of flow rates until breakthrough occurs. A thorough mathematical analysis gives an upper limit approximation for the breakthrough time as

$$T_B = \frac{(n-1) \cdot a_0}{(2n+1) \cdot 2\gamma \cdot F(L,0)} \qquad (2)$$

$\gamma = 1.17 \cdot 10^9$ cm^{3}s year mol^{-1} converts the dissolution rate $F(L,0)$ at the exit of the fracture at $t = 0$ from mol/cm^{2}s to removal of bedrock in cm/year. T_B is given in years. Thus breakthrough occurs, when the aperture width at the exit has increased to several times of its initial value (DREYBRODT 1996, DREYBRODT & GABROVSEK 2000a).

The initial dissolution rates $F(x,0)$ along the uniform initial fracture have been given by DREYBRODT (1996), and also GABROVSEK (2000). Here for understanding of the importance of nonlinear kinetics we shortly discuss the results. Due to dissolution of limestone along the fracture a concentration profile $c(x)$ develops (see Figure 3c, curve 1), where x is the coordinate along the fracture. From this profile the dissolution rates result as

$$F(x,0) = F(0)\,\exp(-x/\lambda) \text{ for } x \leq x_s$$

$$F(x,0) = F(c_s)\,[1 + \frac{(n-1)\,(x-x_s)}{\lambda}]^{-\frac{n}{n-1}} \text{ for } x > x_s. \qquad (3)$$

with

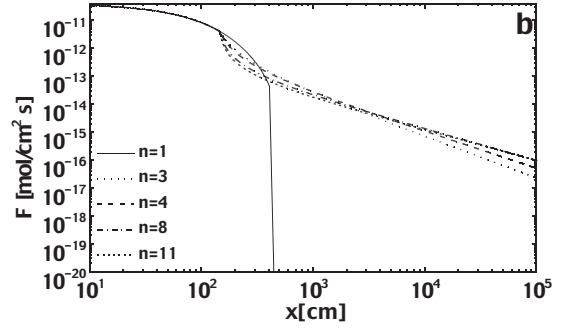$$\lambda = \frac{\rho g}{24\eta} \cdot \frac{a^3 h}{L} \cdot \frac{c_{eq}}{k_n(1-c_s/c_{eq})^{n-1}}$$

Fig. 4. Dissolution rates along the uniform "standard" fracture for various order n of the rate equation as denoted in the figure

x_s is the distance from the entrance where the rate law switches to nonlinear kinetics. The profile $F(x,0)$ of dissolution rates along our uniform initial standard fracture is depicted by Text-fig. 4. Note the logarithmic scales. If the dissolution rates were entirely linear up to equilibrium the full line (n=1) would result. The rates drop steeply by ten orders of magnitude after a short distance of only 4 m and widening of the fracture is restricted to its entrance. Only surface denudation would result. If the rates, however, switch to a nonlinear rate law the decrease in rates switches at x_s from an exponential to a much smoother hyperbolic decline, depicted by the dotted lines for various values of n. Then the rates at the exit are still sufficiently high to obtain breakthrough. This stresses the importance of nonlinear rate laws to large scale karstification. Introducing $F(L,0)$ into eqn. 2 one obtains the breakthrough time T_B as

$$T_B \approx \frac{1}{2\gamma} \cdot \frac{n-1}{2n+1} \cdot \left(\frac{1}{a_0}\right)^{\frac{2n+1}{n-1}} \left(\frac{24\eta L\,(n-1)}{\rho gic_{eq}}\right)^{\frac{n}{n-1}} (k_n)^{\frac{1}{n-1}} \qquad (4)$$

η is the viscosity of the water, ρ its density, and g earth's gravitational acceleration. Using units in [g], [cm], [s], [mole/cm^3] one obtains T_B in years.

This equation specifies breakthrough time as a function of the parameters determining the evolution of karst. Breakthrough time can be regarded as a measure of the degree of karstification in the sense that more highly karstified regions are expected, if breakthrough occurs in shorter times. The consequences of eqn. 4 to the understanding of karstification have been discussed in detail elsewhere (DREYBRODT 1996, DREYBRODT & GABROVSEK 2000, DREYBRODT & SIEMERS 2000). It should be noted here that completely smooth even spaced fractures are an idealization and do not occur in nature. It has been shown, however,

that even considerable natural roughness of the fractures has no significant influence to the general pattern of early karst evolution, and only little influence to the value of the breakthrough time. (DREYBRODT & GABROVSEK, 2000b)

BREAKTHROUGH ON TWO-DIMENSIONAL NETWORKS

Real karst systems are three-dimensional or at least two-dimensional as envisaged by case 2 in Text-fig. 1. To model a two-dimensional net of fractures, we use an empty square lattice and introduce fractures with aperture widths a_0 by a statistical method (SIEMERS &

DREYBRODT, 1998). The resulting network is shown by Text-fig. 5. The net consists of fractures 1 m wide with initial aperture widths of 0.03 cm. The length of each single fracture is 10 m and the total length of the karst aquifer amounts to 3 km. The left hand side contains a variety of input points at a hydraulic head of 150 m, the right hand side exhibits several outputs at a head of zero. The upper and the lower boundaries are impermeable. All other constants are those of the one-dimensional standard fracture discussed in the proceeding chapter.

To model the evolution of karst conduits in such a net one has to couple flow equations and the dissolution programme along the one-dimensional elements of the net (SIEMERS & DREYBRODT 1998).
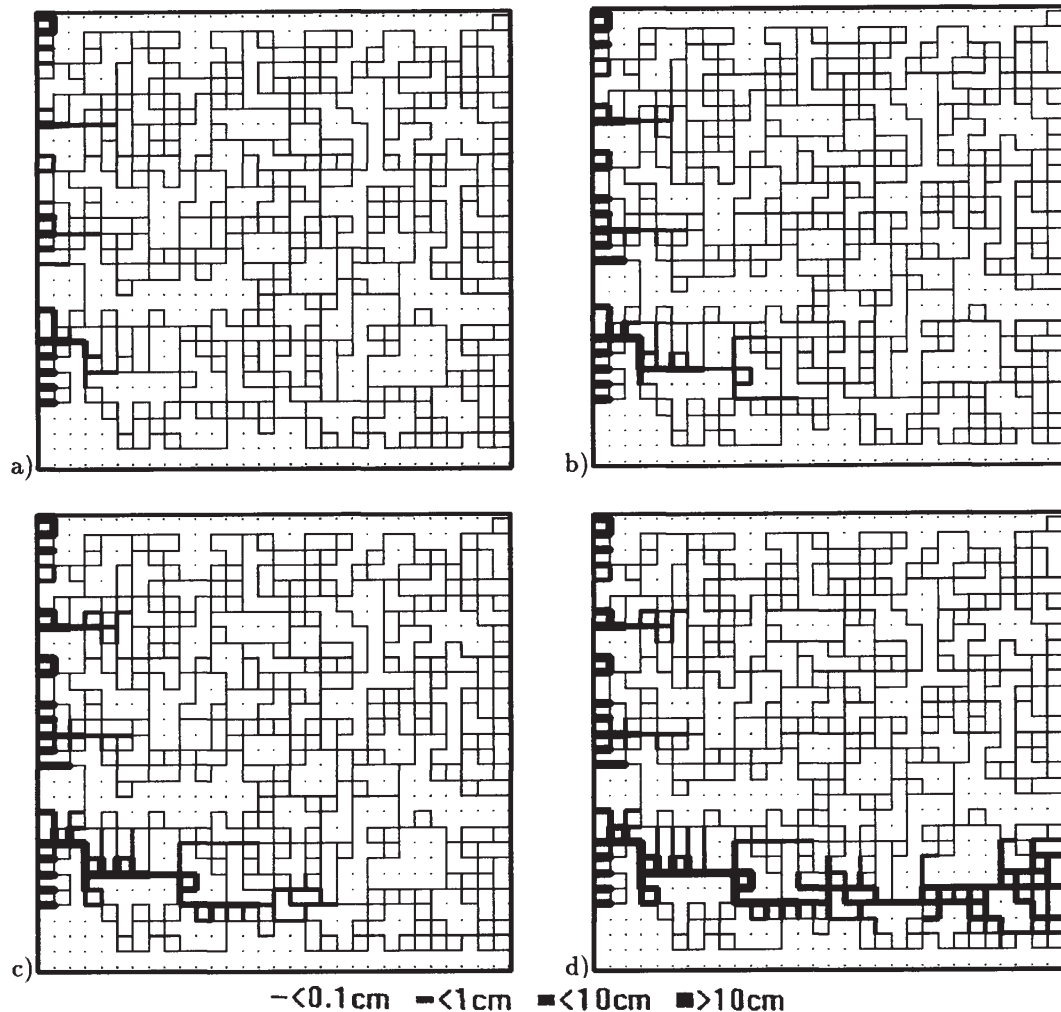

Fig. 5. Evolution of a karst aquifer with $p=0.7$ at 9660 years (a), 13657 years (b), 17362 years (c) and 17762 years (d). The upper and lower boundaries are impervious. The left side boundary is at constant head $h=150$ m, whereas the head at the right side boundary is $h=0$ m. The thickness of the lines represents the average aperture widths of the fractures, with the code: $-< 0.1$ cm; $=< 1$ cm; < 10 cm; > 10 cm. Parameters $a_0=0.03$ cm, $b_0=100$ cm, $h=15000$ cm, $L=3\text{x}10^5$ cm, $n=4$, $c_s=0.9$, $c_{eq}=2\text{x}10^{-6}$ mole cm^{-3}, and $k_4=4\text{x}10^{-8}$ mole cm^{-2}s^{-1}
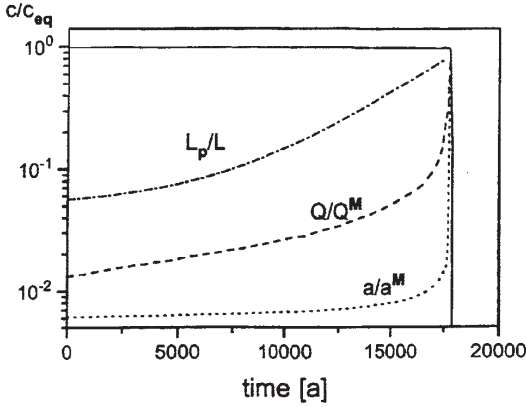
Fig. 6. Evolution of penetration length , flowrate and concentration. At the exit of the winning patway. Q_m and a_m are the values reached at the breakthrough. Q_m =518 cm³s⁻¹, a_m =4.86 cm. At breakthrough the concentration switches to values close to zero

Text-fig. 5 gives an example of the breakthrough behaviour typical for all simulations. The network simulates the initial hydrogeological setting. Figure 5a shows the average widths of the fractures after 9960 years. These average widths are those which a uniform conduit with even spacing $\bar{a}$ would exhibit, if it had the same resistance as the real conduit with a profile $a(x)$. Figure 5b-5c illustrate the further evolution as the conduits penetrate into the system. Finally after 17762 years the first channel has reached an exit point. The distance of penetration $L_p(t)$ can now be defined by the largest distance from the input, where channels have been widened to 0.1cm. Breakthrough at time T_B is achieved when $L_p(T_B) = L$.

Text-fig. 6 shows as a function of time: L_p/L, the width $a(t)/a(T_B)$, the water flow $Q(t)/Q(T_B)$, and the concentration $c(t)/c_{eq}$ of the solution at the breakthrough exit point. All these quantities show a typical breakthrough behaviour. We define the breakthrough time by the time at which the concentration of the water leaving the major exit point drops below $10^{-3}c_{eq}$. In all cases flow was laminar, as checked by calculating the Reynolds number to be below 1000.

NUMERICAL SENSITIVITY ANALYSIS OF BREAKTHROUGH TIME ON TWO-DIMENSIONAL NETS

Using such a network but changing only one of its parameters at a time we have calculated the dependence of the breakthrough time as a function of these parameters. The result is summarised by the following expression

$$T_B = (a_0)^{\frac{2n+1}{n-1}} \cdot \left(\frac{L^2 \eta}{h c_{eq}} \right)^{\frac{n}{n-1}} \cdot k_n^{\frac{1}{n-1}} \cdot c(p,s) \qquad (5)$$

The constant $c(p,s)$ is dependent only on the properties of the initial fracture system. It depends on the occupation probability p of the square lattice by fractures and the geological setting s. This equation resembles closely that of the one-dimensional case (eqn. 4) provided the length l of the conduit is replaced by the spatial dimension L of the fracture system.
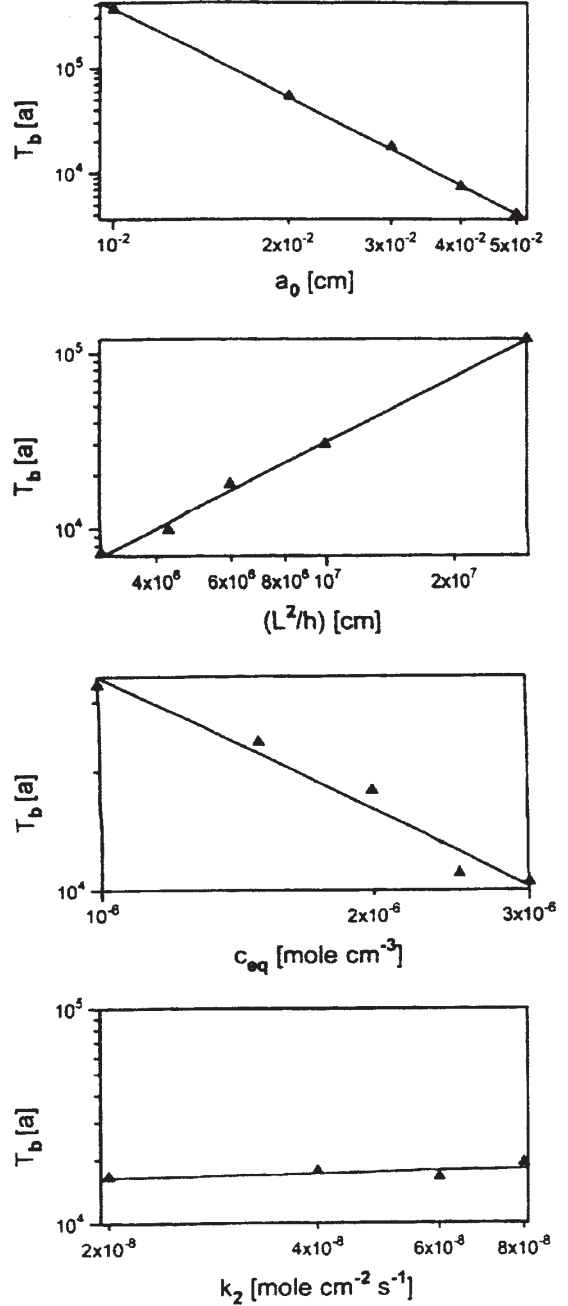

Fig. 7. Double logarithmic plot of breakthrough time as a function of a_0, (L^2/h), c_{eq} and k_4, for $n=4$, $p=0.7$, as obtained from computer runs on the grid of Text-fig. 5

Text-fig. 7 represents a verification of eqn 5. Here we have plotted the breakthrough times calculated for various a_0, L^2/h, c_{eq} and k_4 in a double logarithmic plot as functions of the corresponding variables, whereby we have used results from the fracture system shown in Text-fig. 5. The straight lines plotted through the calculated point show the validity of the power law, and the exponent can be calculated from its slope. The exponents obtained are within % those predicted from eqn. 5. We have also calculated the breakthrough times in their dependence on the various parameters as defined above for a variety of different values of n between $n = 3$ up to $n = 11$ and have found eqn. 5 to be valid in this range. Furthermore we have performed such calculations on a variety of different initial fracture systems with identical boundary conditions and different occupation probabilities. These also have verified the predictions of eqn. 5 (SIEMERS & DREYBRODT 1998).

THE INFLUENCE OF CLIMATE ON BREAK-THROUGH TIMES

As noted already breakthrough times can be regarded as a measure for the intensity of karstification. In any case breakthrough is the indispensable condition for the further evolution to mature karst under conditions of constant recharge. The shorter breakthrough times are the more occasions for further karstification exist.

The two main climatic variables determining breakthrough are temperature and annual precipitation. Precipitation must be sufficient to provide constant head conditions, e.g. lakes or rivers on karst plateaus, to feed water to the inputs. Breakthrough times are dependent on temperature because the viscosity of water depends on temperature, and c_{eq} is also related to the mean annual temperature. The relation between c_{eq} and temperature is complex, because c_{eq} depends also on the carbon dioxide partial pressure in the soil on the karst plateau. The CO_2-pressure, however, is also a complex function of temperature and precipitation (FORD 1989). Therefore we use empirical data on c_{eq} for various climates, as they have been reported by SMITH & ATKINSON (1976) from a large number of water samples in karst regions. Average values of c_{eq} for arctic/alpine climate with average temperature of about 5°C are 0.83 ± 0.35 mmol/l. In temperate climates c_{eq} is high at 2.11± 0.8 mmol/ at about 10°C. Tropical climate exhibits $c_{eq} = 1.74 ± 0.24$ mmol/l at about 25°C. Viscosity of water is reduced by a factor of two, when going from 5°C to 25°C.

By use of these numbers we are able to compare breakthrough times on an otherwise identical geological setting. If such a setting exhibits breakthrough time T for arctic climate, solely due to the empirical temperature dependence of c_{eq} and viscosity it would show a breakthrough time 0.25 T for temperature climate, and T = 0.17 T for tropic climate, respectively. There is also a weak influence owing to the temperature dependence of k_4. But within the accuracy of our estimation this can be safely neglected (see Text-fig. 7).

Our model gives an explanation on the influence of crude climatic variables to karstification. This, however, must not be overestimated since many local variables also take a strong influence to breakthrough times.

THE INFLUENCE OF VEGETATION TO THE EVOLUTION OF KARST CONDUITS

Waters mixing at the confluences of single fractures in a two dimensional karst aquifer can have quite different chemical composition, when the p_{CO_2} in the soil on top of the aquifer shows local variations. If, for example the karst plateau above consists of regions of bare rock and also vegetated areas, waters coming from these distinctly different regions can mix at confluences of various fractures. In this case both waters will be close to equilibrium, but will have different values of c_{eq}. The mixture of such waters shows renewed aggressiveness due to mixing corrosion (BÖGLI 1980, DREYBRODT 1988). GABROVSEK & DREYBRODT (2000) have investigated the consequences to breakthrough times. The most important results are given here, to demonstrate the large impact to karstification.

Text-fig. 8 shows a symmetric confluence of two fractures. Fracture 1 is at hydraulic head h_1, carries flow Q_1 with water of initial $p_{CO_2} = p_1$. Accordingly fracture 2 has head h_2, flow rate Q_2, and $p_{CO_2} = p_2$. The waters mix in the confluence of the two input fractures at position kL, and due to the effect of mixing corrosion the dissolution rates increase drastically. As a consequence also the dissolution rates at the exit must increase and therefore breakthrough times are reduced.
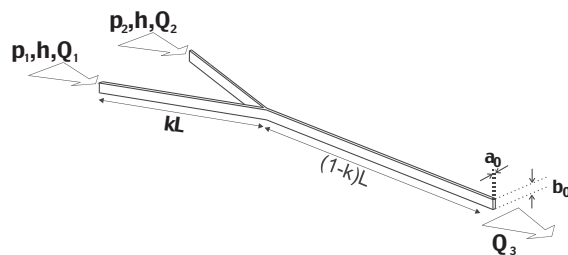

Fig. 8. Symmetric confluence of two fractures. Conceptual model for the most simple scenario where mixing corrosion is active. p_1 and p_2 denote the p_{CO_2} of solutions at the entrances of the fractures which join at the position kL
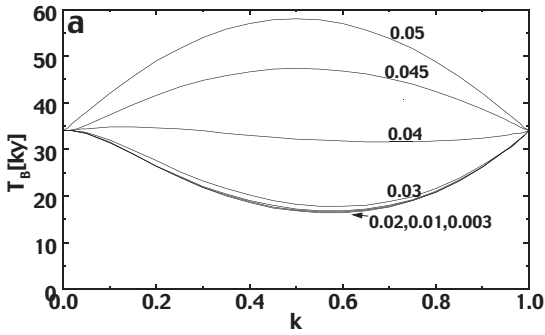
Fig. 9. Breakthrough time as a function of k. p_1=0.05 atm, value of p_2 are denoted on the curves

Text-fig. 9 shows the breakthrough times for a symmetrical confluence ($h_1 = h_2$) in dependence to k. The upper curve results when both inputs have equal p_{CO_2} = 0.05 atm and therefore mixing corrosion is absent. For k = 0 the confluence is at the entrance and therefore we deal with one single conduit. The breakthrough time is therefore single conduit breakthrough time. For k = 1 we have two identical separated conduits joining at their exit. Again the breakthrough time is that of a single conduit. For k ≠ 0 the breakthrough times are higher. The lower curves show breakthrough times, when p_{CO_2} at input 1 is 0.05 atm and at input 2 it is given by the number on the corresponding curve. Mixing corrosion becomes active and consequently the breakthrough times drop. Even small differences in the input p_{CO_2} are sufficient to reduce breakthrough times by a factor of two. At larger differences of p_{CO_2}, e.g. 0.05 and 0.02 atm. respectively, breakthrough times are reduced from 60 ky to 15 ky for k = 0.5. This example shows that individual geochemical settings have a strong influence to the intensity of karstification.

As a further example Text-fig. 10 shows the effect of mixing corrosion to karst evolution on a two-dimensional net. Text-fig. 10a illustrates the evolution of the net at breakthrough time of 16.8 ky. The two inputs at the left hand side both are fed by water with a p_{CO_2} = 0.05 atm and mixing corrosion is absent. In Text-fig. 10b the upper input is at p_{CO_2} = 0.05 atm, but the lower one at 0.03 atm. Mixing corrosion occurs at point A, where widened isolated conduits have been created. Confluence of waters from both inputs occurs also at point B. Therefore enhanced dissolution is active from there to the exit. This causes a reduction of breakthrough time to 8.8 ky. In Text-fig. 10c the lower input is changed to atm, which corresponds to a bare rock surface. Due to the low the evolution of the karst channel from this input is inhibited, but at the points A and B of the confluence mixing corrosion becomes more pronounced. From point A a large conduit has propagated,
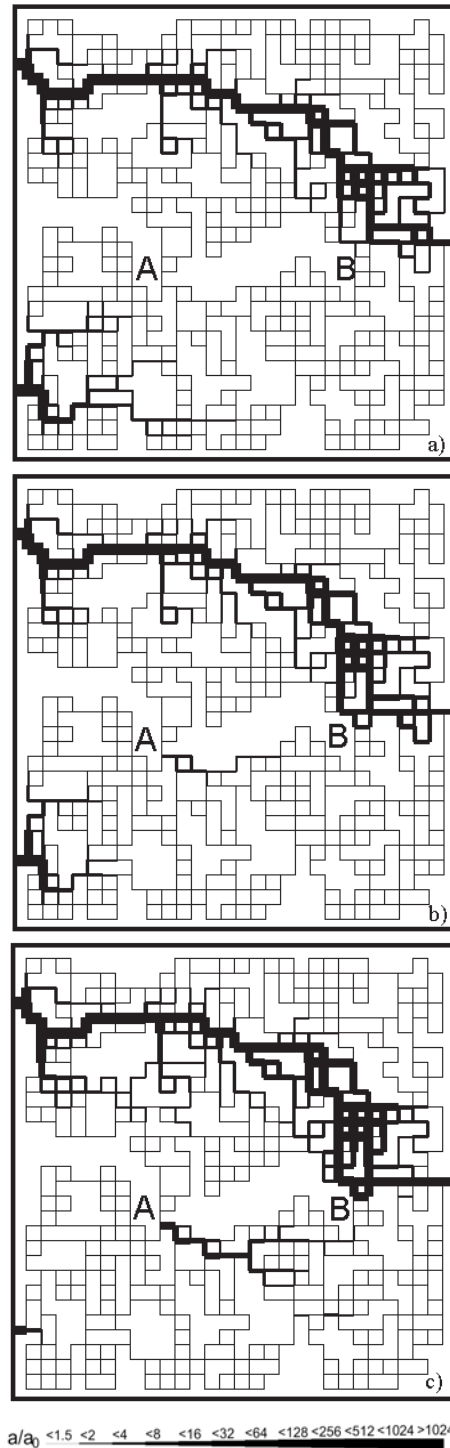

Fig. 10. Aperture widths at breakthrough on a percolation net with P=0.7. All other parameters as in Text-fig. 1. at the upper input is 0.05 atm. **a** – at lower input 0.05 atm, no MC active, T_B=16.8 ky. **b** – at lower input is 0.03 atm, T_B=8.8 ky, **c** – at lower input is 0.003 atm, T_B=5 ky. The fracture aperture widths are represented by the thicknesses of the lines in a geometrical progression as indicated

creating an entrance-less cave. Breakthrough time is now reduced to 5 ky. This example shows that micro-climatic conditions exert influence to karstification similar to that of large scale climate.

CONCLUSION

We have presented models of early karstification under conditions of constant heads at the input and at the output of evolving karst conduits. From both one-dimensional and two-dimensional models the parameters are derived, which determine breakthrough time. At that time the conduits have widened to such an amount, that constant head conditions are no longer sustained and the aquifer switches to conditions of constant recharge.

The parameters determining breakthrough time are those of the hydrologic setting, i.e. the aperture widths of the initial fractures, their length, and the hydraulic head acting along them, and the viscosity of water, which depends on temperature. A second set of parameters is related to the dissolution kinetics. These parameters are the rate constants, and the equilibrium concentration of Ca with respect to calcite. The latter value is influenced significantly by climatic conditions. Breakthrough times can be regarded as a measure of intensity of karstification. They are under otherwise identical geological settings largest for arctic/alpine climate and are lower by about a factor of four to five for temperate and tropical climate, respectively. Micro-climatic conditions which determine the vegetation on karst plateaus exert similar influence. Differences in p_{CO_2} of the waters entering the aquifer cause renewed aggressiveness of the water by mixing corrosion, when such chemically different waters mix. This impact can reduce breakthrough time significantly in comparison to uniform p_{CO_2} at the karst plateau. In conclusion although climatic conditions play an important role in karstification, it seems not to be possible to draw conclusions about climate during early karstification in retrospective.

REFERENCES

BÖGLI, A. 1980. Karst hydrology and physical speleology. *Springer*; Berlin.

CLEMENS, T., HÜCKINGHAUS, D., SAUTER, M., LIED, R. & TEUTSCH, G. 1997. Modelling the genesis of karst aquifer systems using a coupled reactive network model. *In*: Hard Rock Geosciences. *IAHS Publication*, pp. 1-241, Colorado, 3-10.

DREYBRODT W. 1988. Processes in karst systems - Physics, Chemistry and Geology. *Springer Series in Physical Environments,* **4**. *Springer*; Berlin – New York.

— 1990. The role of dissolution kinetics in the development of karstification in limestone: A model simulation of karst evolution. *Journal of Geology*, **98**, 639-655.

— 1996. Principles of early development of karst conduits under natural and man-made conditions revealed by mathematical analysis of numerical models. *Water Resources Research*, **32**, 2923-2935.

— 2000. Equilibrium Chemistry of karst water in limestone Terranes. *In*: KLIMCHOUK, A., FORD, D.C., PALMER, A.N. & DREYBRODT, W. (*Eds*), Speleogenesis: Evolution of karst aquifers. *National Speleological Society*, USA.

DREYBRODT, W. & EISENLOHR, L. 2000. Limestone dissolution rates in karst environments. *In*: KLIMCHOUK, A., FORD, D.C., PALMER, A.N. & DREYBRODT, W. (*Eds*), Speleogenesis: Evolution of karst aquifers. *National Speleological Society*, USA.

DREYBRODT, W. & GABROVSEK F. 2000a. Dynamics of the evolution of a single karst conduit. *In*: KLIMCHOUK, A., FORD, D.C., PALMER, A.N. & DREYBRODT, W. (*Eds*), Speleogenesis: Evolution of karst aquifers. *National Speleological Society*, USA.

— & — 2000b. Influence of fracture roughness on karstification. conduit *In*: KLIMCHOUK, A., FORD, D.C., PALMER, A.N. & DREYBRODT, W. (*Eds*), Speleogenesis: Evolution of karst aquifers. *National Speleological Society*, USA.

DREYBRODT, W. & SIEMERS, J. 2000. Cave evolution on two-dimensional networks of primary fractures in limestone. *In*: KLIMCHOUK, A., FORD, D.C., PALMER, A.N. & DREYBRODT, W. (*Eds*), Speleogenesis: Evolution of karst aquifers. *National Speleological Society*, USA.

EISENLOHR L., METEVA, K., GABROVSEK, F. & DREYBRODT, W. 1999. The inhibiting action of intrinsic impurities in natural calcium carbonate minerals to their dissolution kinetics in aqueous $H_2O\text{-}CO_2$ solutions. *Geochimica Cosmochimica, Acta*, **63**, 989-1002.

FORD, D.C., 1971 Geological Structure and a new explanation of limestone cavern genesis. *Cave Research Group of Great Britain, Transactions*, **13**, 81-94.

— 1999. Perspectives in karst hydrogeology and cavern genesis. *In*: PALMER, A.N., PALMER, M. & SASOVSKY, I.D. (*Eds*), Karst modeling, *Karst Waters Institute*, Charles Town, West Virginia, USA, pp. 17-29.

FORD, D.C. & EWERS, R.O. 1978. The development of limestone caves in the dimensions of length and depth. *Canadian Journal of Earth Sciences*, **15**, 1783-1798.

FORD, D.C. & WILLIAMS, P.W. 1989. Karst geomorphology and hydrology. *Unwin Hyman*; London.

GABROVSEK, F. 2000. Evolution of early karst aquifers. From simple principles to complex models. *Založba ZRC, SAZU*, 150 pp. Ljubljana.

GABROVSEK, F. & DREYBRODT, W. 2000. A model of early evolution of karst conduits affected by subterranean CO_2 sources. *Environmental Geology*. **39**, 531-543.

— & — 2000. The role of mixing corrosion in calcite aggressive $H_2O\text{-}CO_2\text{-}CaCO_3$ solutions in the early evolution of karst aquifers. *Water Resources Research,* **5**, 1179-1188.

GROVES, C.G. & HOWARD, A.D. 1994. Early development of karst systems. 1. Preferential flow path enlargement under laminar flow. *Water Resources Research*, **30**, 2837-2846.

HOWARD, A.D. & GROVES, C.G. 1995. Early development of karst systems 2. Turbulent flow. *Water Resources Research*, **31**, 19-26.

KAUFMANN, G. & BRAUN, J. 1999. Karst aquifer evolution in fractured rocks. *Water Resources Research,* **35**, 3223-3238.

— & — 2000. Karst aquifer evolution in fractured, porous rocks. *Water Resources Research*, **36**, 1381-1392.

PALMER, A. N. 1984. Recent trends in karst geomorphology. *Journal of Geological Education*, **32**, 247-253.

— 1991. The origin and morphology of limestone caves. *Bulletin of the Geological Society of America*, **103**, 1-21.

— 2000. Digital modeling of individual solution conduits. *In*:

KLIMCHOUK, A., FORD, D.C., PALMER, A.N. & DREYBRODT, W. (*Eds*), Speleogenesis: Evolution of karst aquifers. *National Speleological Society*, USA.

RHOADES, R. & SINACORI, M.N. 1941. The pattern of groundwater flow and solution. *Journal of Geology*, **49**, 785-794.

SIEMERS, J. & DREYBRODT, W. 1998. Early development of karst aquifers on percolation networks of fractures in limestone. *Water Resources Research*, **34**, 409-419.

SMITH, D.I. & ATKINSON, T.C. 1976. Process, landforms and climate in limestone regions. *In*: DERBYSHIRE, E. (*Ed.*), Geomorphology and Climate. *John Wiley and Sons*; London

SVENSSON, U. & DREYBRODT, W. 1992. Dissolution kinetics of natural calcite minerals in CO2 -water systems approaching calcite equilibrium. *Chemical Geol*ogy, **100**, 129-145.

SWINNERTON, A.C. 1932. Origin of limestone caverns. *Geological Society of America Bulletin*, **34**, 662-693.

WHITE, W.B. 1977. The role of solution kinetics in the development of karst aquifers. *In*: TOLSON, J.S. & DOYLE, F.L. (*Ed*.) *UAH-Press*; Huntsville, Alabama, USA.

— 1988. Geomorphology and hydrology of karst terrains. *Oxford University Press*; New York